It is noted that once again the strong spin-orbit interaction in InSb is responsible for an important nonlinear optical use of the material. First, the presence of the interaction leads to valence-band eigenfunctions of mixed spin and so to the existence of spin-flip Raman scattering. Second, the strength of the interaction yields a high g^* value with a correspondingly large Raman tuning range, and, most importantly here, produces a relatively large magnetic-dipole spin-resonance transition strength. Also the long lifetime of the spin-down state is essential to the strengths of the peak Raman emission (important for the achievement of Raman oscillation) and the difference mixing coefficient.

ACKNOWLEDGMENT

The authors wish to thank Prof. S. D. Smith, for encouraging this investigation of far-infrared generation and for constructive comments during the work, and M. Kimmitt of Essex University for provision of the Ga:Ge detector.

REFERENCES

[1] V. T. Nguyen and T. J. Bridges. "Resonant optical nonlinearity due to conduction-electron spins in InSb," *Phys. Rev. Lett.*, vol. 29, pp. 359–361, Aug. 1972.
[2] T. J. Bridges and V. T. Nguyen, "Generation of tunable far-infrared radiation by difference frequency mixing using conduction electron spin nonlinearity in InSb," *Appl. Phys. Lett.*, vol. 23, pp. 107–109, July 1973.
[3] T. L. Brown and P. A. Wolff, "Theory of resonant, far-infrared generation in InSb," *Phys. Rev. Lett.*, vol. 29, pp. 362–364, Aug. 1973.
[4] C. R. Pidgeon and S. H. Groves, "Inversion-asymmetry and warping-induced interband magneto-optical transitions in InSb," *Phys. Rev.*, vol. 186, pp. 824–833, Oct. 1969.
[5] B. S. Wherrett and C. R. Pidgeon, "Electric dipole contributions to resonant far-infrared differency-frequency mixing in InSb," *Phys. Rev. B.*, vol. 9, pp. 711–715, Jan. 1974.
[6] B. S. Wherrett, S. Wolland, C. R. Pidgeon, R. B. Dennis, and S. D. Smith, in *Proc. 12th Int. Conf. Semiconductor Physics* (Stuttgart, Germany), 1974, to be published.
[7] N. Brignall, R. A. Wood, C. R. Pidgeon, and B. S. Wherrett, *Opt. Commun.*, to be published.

Far-Infrared–Submillimeter Phased Arrays and Applications

VINCENT J. CORCORAN, MEMBER, IEEE

***Abstract*—The concept of a phased array of far-infrared (FIR) or submillimeter (SMM) waveguide lasers that can be scanned electronically is presented. Grating lobe reduction by computer analysis is shown. Possible applications of SMM arrays are considered.**

I. INTRODUCTION

WAVEGUIDE laser action has been demonstrated in the far-infrared (FIR) region in both electrical discharge lasers [1] and optically pumped lasers [2]. These waveguide lasers provide a high energy density source of coherent radiation, and are important components for phased arrays of lasers in the FIR and submillimeter (SMM) regions. These phased arrays can be electronically scanned so that high energy density radiation may be rapidly moved in space to a desired point. This paper is concerned with illustrating the array concept and the problems associated with the concept. The analytical results of a technique to reduce the grating lobe problem are presented. Applications of arrays in the SMM region are considered based on the atmospheric characteristics in this region.

Manuscript received August 26, 1974.
The author is with the Institute for Defense Analyses, Arlington, Va. 22202.

II. ARRAY CONCEPT

The electronically scanned laser array employs rows and columns of FIR or SMM waveguide lasers and electrooptic phase modulators as shown in Fig. 1. Each laser output passes through a modulator which adjusts the phase of a laser beam relative to another. Optical feedback from the lasers is used to injection lock one laser to another so that the relative phase of each laser is constant. The inputs to the modulators then control the relative phase of the elements of the array. The phase shifting can be used to move the beam in space by adjusting the phase of each laser modulator electronically. In this way a rapid scan can be achieved, since the response time of an electrooptic modulator is very fast compared to mechanical scanning.

Although the device as described earlier can be used to scan, its accuracy is impeded by the possibility of drift in frequency of the laser. This can be overcome by the extension of the phase lock technique described for the HCN laser [3]. With this method a signal is multiplied from a standard frequency to the frequency of the laser. This signal is used as a reference for a phase detector so that that error between the laser phase and the reference is used as an error signal to correct the phase of the laser through the laser power supply. As a result, an absolutely

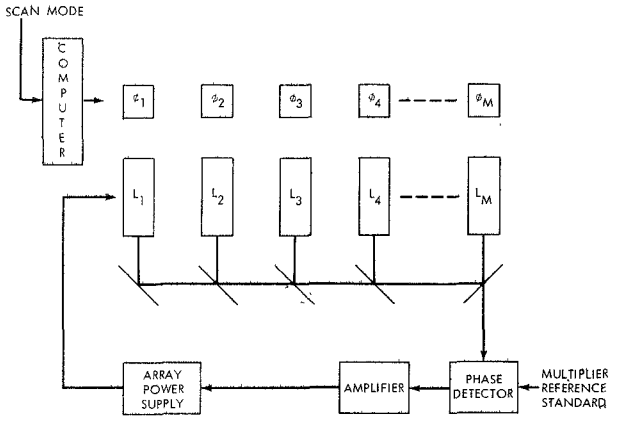

Fig. 1. Transmitter detail showing injection locking lasers, phase locking of the laser array to a frequency standard through the power supply, and scanning effected by driving phase modulators through a computer.

stable laser signal which can be adjusted in phase can be used as an element in a scanned array since each element is properly phased to each other through injection locking and phase modulation.

An SMM waveguide laser with a 10-mm bore diameter can produce milliwatts of average power and kilowatts of peak pulsed power at this time. A 100×100 array, therefore, would require a cross section of 1 m^2. As a result, 10^4 times the power of an individual laser could be achieved and since the power gain depends on N^2 for an array, the peak powers in space would be 10^8 times the power of an individual element. These power levels correspond to those achieved with gas dynamic or chemical lasers.

III. ANALYSIS

The laser array described is a highly thinned array where the apertures and the aperture spacings are many wavelengths. If the sources are equally spaced and the aperture spacing is greater than the aperture size, then closely spaced grating lobes exist which would produce signal returns comparable to the main lobe. This problem is circumvented by making the spacing between elements unequal. For example, consider an array with an element at the origin and elements symmetrically located about the origin.

The far field intensity pattern, which is related to the Fourier transform of the aperture pattern, is given by

$$I(\theta) = \left\{\frac{\sin\left[(\pi/\lambda)b \sin\theta\right]}{(\pi/\lambda)\sin\theta} \cdot \left[1 + \sum_{n=1}^{(N-1)/2} 2\cos\left(\frac{2\pi}{\lambda} d_n \sin\theta\right)\right]\right\}^2$$

where

- λ wavelength;
- b aperture width;
- θ angle from the normal to the array;
- d_n distance from the center of array to the center of the nth aperture.

This equation is a product of an aperture function and a grating function. The grating function, the aperture function, and the product are illustrated in Fig. 2 for the case where the elements are equally spaced and the spacing is greater than the aperture. A method for reducing the grating lobes comes from inspection of the grating function; to choose the spacings to be nondegenerate, i.e., the spacings should be such that the grating lobes due to one spacing do not coincide with another set of grating lobes. This occurs when the ratio of any two spacings is not an integer. In this case, the main lobe is N^2, and the grating lobes are down 20 dB from the main lobe for $N = 100$.

A computer program has been used to check the feasibility of reducing the grating lobes as indicated by the preceding equation. When nine elements are used in a linear array, then the computed far field pattern for a symmetric array at 100 μm is given in Fig. 3. It is evident

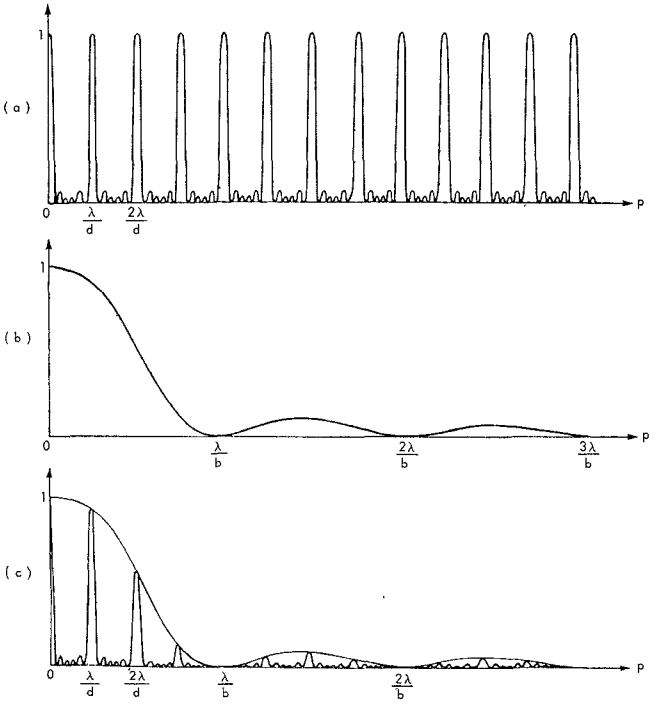

Fig. 2. (a) Illustration of grating function. (b) Aperture function. (c) Product of $a \times b$ for far field pattern.

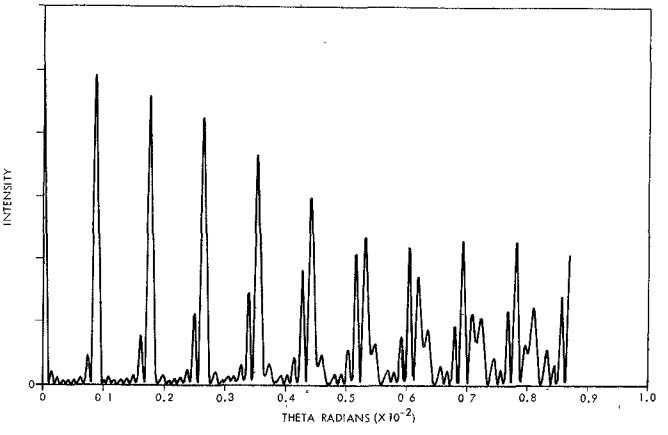

Fig. 3. Computer run for far field pattern of nine element symmetrical array with unequal spacing between elements. $\lambda = 100$ μm, $b = 10$ mm, and $d_n \sim 5$–10 cm.

that, although some grating lobe reduction occurs, the grating lobe reduction is not significant.

The computed far field pattern for a symmetric linear array with 91 elements has been plotted in Fig. 4 for a 100-μm wavelength. Each element has a linear aperture of 10 mm, and the pseudorandom spacing is approximately 10 cm between elements for each of these calculations in order to amplify the grating lobe problem. Despite this exaggeration of the problem, the spacings chosen and the number of elements used result in significant reduction of the grating lobes. Significant improvement could be expected with further judicious choices of separation.

For any array, scanning can be achieved by adjusting the phase of each waveform from an aperture so that the waveforms add at the desired point in space, i.e., so that the optical path length to that point from each aperture is an integral multiple of a wavelength. For the symmetrical array, the objective is to choose path distances such that any pair of elements produce grating lobes spaced differently from any other pair as was done for $\theta = 0$. This can be achieved by choosing the phase adjustment of one element of the nth pair as $\varphi_{n1} = -kd_n \sin\theta$ and the other element as $\varphi_2 = +kd_n \sin\theta$. The intensity is then a maximum at θ. In order to avoid the requirement to maintain the grating lobes at a low level continuously, it may be necessary to use a continguous digital electronic scan rather than a continuous scan.

The total angle over which a phased array can be scanned is limited by the beamwidth of the individual elements. With external optics or by shaping the output optical surfaces of the modulator, the beamwidth can be adjusted to any reasonable angle without difficulty.

For equally spaced elements in a linear phased array, the beamwidth of the array is proportional to $1/N$. For the pseudorandom spacing considered here, the spacings, although unequal, can be made to be approximately equal, if desired. As a result, the assumption that the linear beamwidth is proportional to $1/N$ is reasonable.

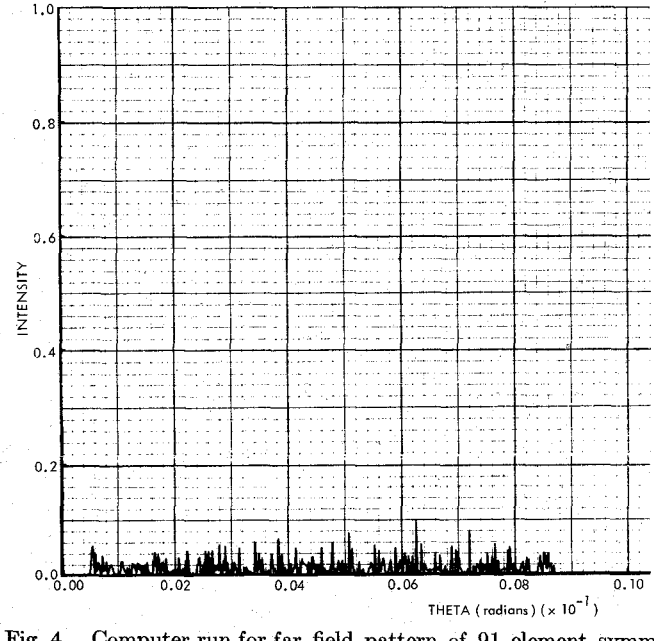

Fig. 4. Computer run for far field pattern of 91 element symmetrical array with unequal spacing between elements. $\lambda = 100$ μm, $b = 10$ mm, and $d_n \sim 5$–10 cm.

The scan rate for a phased array is dependent upon the beamwidth, the total scan angle, and the frame rate. For a linear scan, the relation is

$$\dot{\theta} = (\Omega/\theta) \times \dot{\Omega} = N\dot{\Omega}$$

where

$\dot{\theta}$ scan rate;
Ω total linear scan angle;
θ beamwidth;
$\dot{\Omega}$ frame rate;
N number of elements in the array.

This scan rate is equal to the pulse repetition frequency (PRF) that is required for a continguously scanned pulsed system. For a 100 element linear array and a 30-frame/s rate, the PRF would be 3000 pps.

IV. COMPONENTS

Virtually all of the components and the technology for an electronically scanned phased array in the SMM region have been demonstrated. Laser action in waveguide devices has been shown with an electric discharge and an optical pump. Modulators have been demonstrated at low temperatures. The computer can now be made compact due to the advances of large-scale integration electronics. Low cost optics are readily available in the SMM region. Injection locking of lasers and the absolute stabilization of an SMM laser were demonstrated years ago.

V. ATMOSPHERIC PROPAGATION IN THE SMM REGION

The SMM band is one of the least studied spectral regions for propagating electromagnetic waves; however, sufficient information is available concerning atmospheric effects in this region to permit some general conclusions to be tentatively drawn. The factors that must be considered are not only the transmission properties of the atmospheric gases at sea level, but the effects as a function of altitude and temperature. Also, the influence of high concentration of water vapor as in fogs and water droplets due to clouds and rain must be taken into account. The relative amount of attenuation due to scattering versus absorption is of importance as well.

An investigation of the attenuation coefficients due to atmospheric gases at sea level indicates that large absorption exists from 20 μm to 2 mm even in the relative windows. The absorption is usually determined for an atmosphere that contains a water vapor density of 7.5 g of water per cubic meter of air. Dry atmospheres, of course, produce less attenuation and very humid atmospheres produce more.

The water vapor content also changes as a function of altitude. When this change is taken into account, the propagation through a cloudless atmosphere can be determined. Candidate windows determined by calculations for a zenith path through a cloudless maritime polar atmosphere are given in Table I. The water vapor attenuation for a polar atmosphere is less than for most

TABLE I

CANDIDATE "WINDOWS" IN THE SUBMILLIMETER AND MICROWAVE BANDS, ARISING FROM ABSORPTION SPECTRA OF WATER VAPOR AND OXYGEN, WITH ATTENUATION IN DECIBELS CALCULATED FOR A ZENITH PATH THROUGH A CLOUDLESS MARITIME POLAR ATMOSPHERE [4]

Window	Wavelength (approx.) of window at least gaseous absorption	Bounding Absorption Peaks		Attenuation (in decibels) along zenith path		
		Wavelength of peak absorption	Primary absorbing gas	By water vapor	By oxygen	Combined gaseous absorption
		No absorption of consequence at wavelengths greater than 3.2cm				
I	3.2cm			0.005	0.140	0.145
		1.3cm	Water vapor	0.408	0.200	0.608
II	9mm			0.074	0.340	0.414
		5mm	Oxygen	0.100	135.	135.1
III	3mm			0.253	1.00	1.253
		2.52mm	Oxygen	0.447	30.0	30.447
IV	2.3mm			0.506	0.40	0.906
		1.6mm	Water vapor	65.8	0.18	65.98
V	1.3mm			1.80	0.31	2.11
		920μ	Water vapor	90.9	0.68	91.58
VI	880μ			9.12	0.75	9.87
		780μ	Water vapor	621.	0.95	621.95
VII	720μ			20.9	1.10	22.00
		660μ	Water vapor	874.	1.30	875.30
VIII	650μ			64.8	1.40	66.20
		630μ	Water vapor	184.	1.50	185.50
IX	620μ			55.5	1.55	57.05
		530μ	Water vapor	37,100.	2.10	37,102.
X	490μ			189.	2.40	191.40
		475μ	Water vapor	690.	2.60	692.60
XI	450μ			72.0	2.90	74.90
		397μ	Water vapor	27,000.	3.80	27,003.8
XII	345μ			72.0	5.0	77.0
		325μ	Water vapor	1,450.	5.6	1,455.6
XIII	320μ			189.	5.8	194.8
		303μ	Water vapor	176,000.	6.5	176,006.5
XIV	290μ			360.	7.	367.
		256μ	Water vapor	187,000.	9.	187,009.
XV	237μ			540.	11.	551.
		215μ	Water vapor	176,000.	13.	176,013.
XVI	200μ			486.	15.	501.
		174μ	Water vapor	6,900.	(20.)	6,920.
XVII	164μ			1,230.	(22.)	1,252.
		156μ	Water vapor	6,900.	(25.)	6,925.

TABLE II

PROPORTION OF TOTAL ATTENUATION DUE TO A 500-M STRATO-CUMULUS CLOUD (ZENITH PATH) [4]

Candidate windows		Total gaseous absorption	Contribution by droplets in a 500-meter st-cu cloud	Total attenuation due to gases and cloud droplets	Proportion of total attenuation due to cloud droplets
Window	Wavelength λ				
III	3mm	1.25 db	0.97 db	2.22 db	43.7 %
IV	2.3mm	0.91 db	1.17 db	2.08 db	56.2 %
V	1.3mm	2.11 db	1.60 db	3.71 db	43.2 %
VI	880μ	9.87 db	2.40 db	12.27 db	19.6 %
VII	720μ	22.0 db	2.92 db	24.92 db	11.7 %
IX	620μ	57.0 db	3 00 db	60 0 db	5.0 %
XII	345μ	77.0 db	5.50 db	82.5 db	6.7 %

TABLE III

PROPORTION OF TOTAL ATTENUATION DUE TO MODERATE RAIN OF 2-KM DEPTH (ZENITH PATH THROUGH 500-M STRATO-CUMULUS CLOUD) [4]

Candidate windows		Total gaseous absorption plus contribution to attenuation by 500-meter st-cu cloud	Contribution by moderate rain of 2 km depth	Total attenuation due to gases, cloud and rain	Proportion of total attenuation due to 2 km rain
Window	Wavelength λ				
III	3mm	2.22 db	5.2 db	7.42 db	70 %
IV	2.3mm	2 08 db	2 5 db	4.58 db	55 %
V	1.3mm[a]	3 71 db	2.5 db	6.21 db	40 %
VI	880μ[a]	12 27 db	2.4 db	14.67 db	16 %
VII	720μ[a]	24 92 db	2 3 db	27.22 db	8 %
IX	620μ[a]	60 0 db	(2.2) db	(62.2) db	(3 5)
XII	345μ[a]	82 5 db	(2 0) db	(84.5) db	(2.3)

[a] No allowance made at these wavelengths for possible reduction in attenuation due to moderate rain by the mechanism of forward scatter.

Note: Values in parentheses are extrapolated.

other atmospheres because of the low water vapor content at low temperatures. A tropical atmosphere would produce considerably more attenuation.

Water droplets are found in rain and clouds. These droplets have a distribution of sizes and they produce different effects from water vapor as far as attenuation of electromagnetic waves is concerned. The effects of water droplets in a 500-m strato-cumulus cloud and in moderate rain are given in Tables II and III, respectively, for candidate windows in the millimeter and SMM regions.

In addition to the factors mentioned that contribute to the attenuation of electromagnetic waves, an additional

factor must be considered for maritime atmospheres. It is the water vapor that arises from evaporation at the air–sea interface as a result of turbulent mixing. The increase in attenuation along a zenith path due to this water vapor is approximately 10 percent at any wavelength in the 345-μm–1.3-mm region.

It should be noted that the results given earlier are due to absorption. The attenuation due to scattering is virtually nonexistent in the SMM region by comparison.

Table II indicates that the attenuation due to clouds is approximately equal to or less than that due to gases in the 350-μm–2-cm range. For wavelengths less than 100 μm the attenuation probably rises sharply.

The attenuation due to moderate rain is virtually constant for wavelengths shorter than 3 mm and is less than that due to atmospheric gases.

Attenuation due to moderate rain versus clouds is larger at wavelengths longer than 2.5 mm becoming an order of magnitude greater at 5 mm, and is smaller at shorter wavelengths becoming an order of magnitude less at 400 μm. At wavelengths shorter than 400 μm, the attenuation due to clouds rises rapidly while the attenuation due to rain falls very slowly. The asymptotic high for cloud attenuation occurs at approximately 3 μm and the attenuation due to rain reaches an asymptotic low at approximately 20 μm.

As a rule of thumb, the water droplet population in a 500-m-deep strato-cumulus cloud produces an order of magnitude change in attenuation compared to atmospheric gases. The same is true for rain in the 1.3–2-mm region. At wavelengths greater than 2.5 mm, the attenuation is the dominant factor and for wavelengths less than 720 μm, the rain attenuation is an order of magnitude less and two orders of magnitude less for wavelengths shorter than 400 μm.

Finally, the increase in attenuation due to additional water vapor evaporated into the atmosphere will be approximately 10 percent over the original attenuation in a zenith path through a cloudless atmosphere.

VI. APPLICATIONS

From the data that have been presented on atmospheric transmission, it should be evident that the applications for SMM waves are rather limited other than for use as scientific tools. System applications may exist where the water vapor content is low as at high altitude or in space. Other applications would be limited to relatively short range in the atmosphere.

Applications in space would appear to be the most likely candidates for success. Satellite-to-satellite or satellite-to-space radars would not be hampered by atmospheric condition, and could, therefore, be considered solely on technical merits. Here the SMM systems would provide beamwidth advantages over microwaves and would not require the stringent steering and pointing accuracy of the infrared. Disadvantages as source efficiency would have to be overcome to be competitive.

Because of the decrease in water vapor at higher altitudes, SMM systems could provide advantages in ground-to-space applications where the radar was located at a high altitude site. In this application, efficiency would not be a major consideration and the previously mentioned advantages would apply.

Air-to-air use of SMM waves also would not be subject to the large attenuation that applies at ground level. The lack of scattering of SMM waves would provide for a system whose radiation would be relatively undetectable at lower altitudes when employed in an air-to-air application.

Short range applications could include aircraft landing systems, ship warning systems, and low angle track-while-scan radars for short ranges. Such systems could perform under most weather conditions and they would be difficult to detect because of the lack of scattering and because of severe attenuation at long ranges. Another advantage exists because of the very low backscatter from the sea or terrain at SMM wavelengths.

In order to obtain an understanding of the implications of these results, one can consider a specific example of a linear array containing 100 elements with a scan angle of 10°. Since the beamwidth is 0.01 of the total angle, the beamwidth would be approximately 2 mrad. For a 1-W CW laser the peak intensity becomes 10^4 W, while for a 10-kW pulsed laser the value is 10^8 W. The required pulse repetition frequency for a 1/30-s frame time is 3 kHz.

These numbers are comparable to those attainable with chemical or gas dynamic lasers in the infrared region. The laser array, however, offers the advantages of low power density at the source because the outputs are essentially in parallel. Also, a high degree of coherence in a single mode is possible, which may not necessarily be possible with gas dynamic lasers or chemical lasers. The waveguide lasers can be sealed so that no fuel or exhausts are necessary. The rapid scan rates possible are not attainable with large mirrors that are used at high power levels in gas dynamic lasers and chemical lasers. Finally, this system eliminates the need for large optics and optics that must be capable of withstanding high power levels, while retaining their optical characteristics.

REFERENCES

[1] H. Steffen and F. K. Kneubühl, "Dielectric tube resonators for infrared and submillimeter wave lasers," *Phys. Lett.*, vol. 27A, pp. 612–613, Sept. 1968.
[2] D. T. Hodges and T. S. Hartwick, "Waveguide laser for the far infrared (FIR) pumped by a CO_2 laser," *Appl. Phys. Lett.*, vol. 23, pp. 252–253, Sept. 1973.
[3] R. E. Cupp, V. J. Corcoran, and J. J. Gallagher, "Line narrowing in a phase-locked laser," *IEEE J. Quantum Electron.* (Corresp.), vol. QE-6, pp. 241–243, Apr. 1970.
[4] Study 61, "Penetrability of haze, fog, clouds, and precipitation by radiant energy over the spectral range 0.1 micron to 10 centimeters," Naval Warfare Group, Center Naval Analyses, Arlington, Va., 1969.